https://doi.org/10.1016/j.tre.2021.102265

An evaluation framework of automated electric transportation system

ABSTRACT

Automated Electric Transportation (AET) is an innovative concept that aims to integrate energy, vehicle, highway, and communication infrastructures. It provides an electrified transportation system to support in-motion energy transfer through wireless charging of inductive coupling in the highway. A considerable body of previous research has sought to understand and improve the cooperative vehicle and existing infrastructure system. This research is one of the few studies that propose the frameworks that aim to simultaneously deal with both recent advances in vehicle automation and electrified highways to increase overall transportation system performance. The objective of this study is to develop an evaluation framework of the AET system. It focuses on three measures of effectiveness (MOEs): i) the system capacity, ii) energy savings, and iii) environmental emission reduction. They are examined based on simulated vehicle activity profiles. Results are provided to illustrate the performance of the system capabilities. Our results also contribute to an understanding of the key factors that can increase AET performance, and potentially impacts on future transportation mobility and sustainability.

Keywords: Automated Electric Transportation; Electric Vehicle; Evaluation Framework; Simulation

1. Introduction

The transportation system is an essential backbone for supporting the individual and industrial activities as well as economic developments. In the United States, the transportation sector alone accounts for almost one third (30%) of total energy use, and is second only to the industrial sector (34%) (EIA, 2019a). According to U.S. Energy Information Administration (EIA) (EIA, 2019b), American road vehicles including autos, buses, and trucks consume about 391 million gallons of gasoline per day, equating to approximately 61% of the total oil consumption in this country. They are also responsible for 24% of the nation's greenhouse gas emissions (EPA, 2019). Consequently, various strategies to address the energy and environmental issues will require significant reductions from the transportation sector. For example, a vast and growing body of research focuses on clean and renewable energy, biodiesel, fuel-efficient cars, and so on. They share the common goal to reduce our dependency on foreign energy, and support energy independence. Energy independence will be achieved when American drivers have the choice to power their cars and trucks with non-petroleum fuels (American Energy Independence, 2019). The U.S. Secretary of Energy (American Energy Independence, 2019) emphasized that *energy independence* means changing how we power our cars and trucks from foreign oil to new American-made fuels and batteries.

Automated Electric Transportation (AET) is one concept that would assist in reducing society's dependence on petroleum, reduce our greenhouse production, and aid in meeting the need to rehabilitate our surface transportation infrastructure (Heaslip et al., 2011). AET represents a new approach for surface transportation that addresses the major challenges associated with automobile dependency: energy, capacity, safety, and emissions. AET proposes an electrified freeway system supporting in-motion energy transfer that will overcome challenges of electric vehicles (EVs), including battery weight, cost, and range. Additionally, evolution from human guided to automated vehicles has the potential to significantly increase freeway capacity through more efficient use of available roadway surfaces and higher speeds (Fagnant and Kockelman, 2015; Mahmassani, 2016; Ghiasi et al., 2017; Liu et al., 2017).

AET is a revolutionary example of a *cooperative transportation system*, which combines recent advances in vehicle automation and electric power transfer. AET is an emerging concept for a network of vehicles that control themselves as they traverse from an origin to a destination while being electrically powered in motion - all without the use of connected wires. AET suggests that electrification will extend beyond delivering energy to on-board batteries of stationary vehicles to include technologies that deliver energy on-demand and in real time to moving vehicles. The basic idea is to make the roadway itself a potential source of energy. Unlike the traditional charging system for the EVs, AET introduces a new way to continuously electrify the highway networks by transferring the electricity via wireless power transfer (WPT) pads (Li and Mi, 2014). WPT pads are embedded along the roadway, so that EVs can continue operating without the need of stopping to recharge the batteries at charging stations. This dynamic wireless charging concept was proposed as early as the 1990s by California's Partner for Advanced Transit and Highways (PATH) (PATH, 1996). Since then, numerous studies have been conducted to improve and verify the feasibility of the innovation (e.g., Covic et al., 2000; Boys et al., 2002; Huang et al., 2009; Huh et al., 2011; Choi et al., 2013; Cirimele et al., 2014; Chen et al., 2015; Fuller, 2016; Chen et al., 2018). The Korea Advanced Institute of Science and Technology (KAIST) in South Korea developed an online electric vehicle (OLEV) system that utilizes dynamic wireless charging technology (Jang, 2018), and implemented it in the KAIST campus shuttle system (Suh et al., 2011). Utah State University constructed an electrified test track and demonstrated that in-motion electric vehicles could be effectively and safely charged through dynamic wireless charging (Morris, 2015; Limb et al., 2016; Liu and Song, 2017; Liu et al., 2017). The goal of AET is to offer roadway transportation that is safer, cleaner, faster, more comfortable, and less congested (Freckleton et al., 2011). To achieve this, AET controls a group of vehicles traveling together as a *platoon*, and interacting between vehicles and platoons in a cooperative manner to maximize safety, capacity, and to meet individual travel needs.

In order to understand the benefits of an AET system, the fundamental question underlying this research is: *what are the potential benefits that can be achieved due to advanced technology and platooning strategies in an AET system?* To assess the potential benefits of AET, this requires using techniques to

develop models that will replicate AET technological feasibility, models of how increased technology can improve capacity, reduce energy consumption, and energy-related emissions. The objective of this research is to develop an evaluation framework of the AET system. It focuses on three measures of effectiveness (MOEs): i) the system capacity, ii) energy savings, and iii) environmental emission reduction. This paper aims to provide valuable information concerning how evaluations should be conducted, the methods, and discussion of approaches for conducting those studies. The evaluation framework is crucial and could be further used as the guideline for the newly introduced concepts or systems because it could assist decision makers to evaluate the impacts of AET systems and results could be used to communicate with the public. This paper is divided into five sections. Section 2 provides a review of the AET system, its concepts and configuration. Section 3 explains the evaluation framework of AET system, focusing on the three MOEs. Section 4 presents the analysis and findings. Finally, we conclude and discuss the findings and future research direction in section 5.

2. AET system: concept and overview

AET is a step beyond current state-of-the-art projects such as the Connected Vehicle Program and current electric vehicles. The basic idea behind AET involves the utilization of wireless energy and data transfer technology. Using the dynamic wireless charging technology, such as the one developed by KAIST (Suh et al., 2011) or Utah State University (Limb et al., 2016), road infrastructure can be upgraded to electrified highway networks without the need for overhead wires or third rails. The recent development of electric vehicle and roadway research has been growing rapidly over the past decade at the Center for Sustainable Electrified Transportation (SELECT), Utah State University (USU). Facility and test track with 750 kVA service, a 5,000 square foot vehicle systems integration high-bay building, 20kW solar array, 100kWh energy storage, and a quarter-mile electrified track have been recently constructed within the university area. The facility includes unique capabilities for full-scale integration of vehicle and roadway technologies including in-motion and stationary wireless charging roadway infrastructure, supporting a number of advanced automated transportation research projects (SELECT, 2020).

Figure 1a provides an illustration of the concept of AET, Vehicle-to-Infrastructure (V2I) and Vehicle-to-Vehicle (V2V) automated navigation of AET. The "*automated electric vehicles*" within the AET system possess connected-vehicle capability, which enables vehicle platooning. Automatically adjusting vehicle travel according to the information provided by the V2V/V2I data transfer also has significant potential in enhancing the capacity of the AET system as well as reducing the energy consumption of AET vehicles. It allows vehicles to safely narrow the headway spacing between them while maintaining consistent speeds, thereby allowing vehicles to travel in tight platoons (Freckleton et al., 2011). Lane capacity may be significantly increased by reducing the headway spacing, increasing traveling speeds, and narrowing lane widths. This is especially significant for locations with right-of-way limitations. More throughputs per lane and more lanes without having to physically expand the roadway represent significant motivations for the development of an automated system. The "*drafting effect*" (i.e., a technique where two vehicles or more align in a closing manner in order to reduce the overall effect of drag caused by the front vehicle's slipstream) created would also reduce aerodynamic drag for follower vehicles, thus reducing the amount of energy required to power a vehicle along its path (Browand et al., 1996). It has been shown by field experiments that the average reduction of fuel consumption per vehicle can reach up to 10% when the inter-vehicle distance is around 10 meters (McAuliffe et al., 2017). Furthermore, recent technological advancements in wireless power transfer (WPT) enable an alternative way to power the in-motion vehicles. WPT concept for AET system is depicted in Figure 1b. The key is to use a magnetic field that induces power across an air gap to a load without physical contact. With this technology, the roadway itself essentially becomes a charging station, and thus allowing for a substantial increase in electric vehicles' range. In addition, for EV users, this technology can add convenience as they can travel longer without requiring a long recharging stop. In this study, we only consider dynamic wireless charging facilities. Jointly using dynamic wireless charging lanes and charging stations along highway corridors

might bring more benefits to electric vehicle users. Charging lanes provide a more convenient charging service than charging stations but might require higher charging costs. Chen et al. (2017) found that charging lanes are competitive as compared with charging stations for attracting electric vehicle drivers with a high value of time. The efficiency and cleanliness of conversion of fossil fuel sources to electric energy for the vehicle can be achieved. For details of concepts and configuration, please refer to works done by (Heaslip et al., 2011; Freckleton et al., 2011).

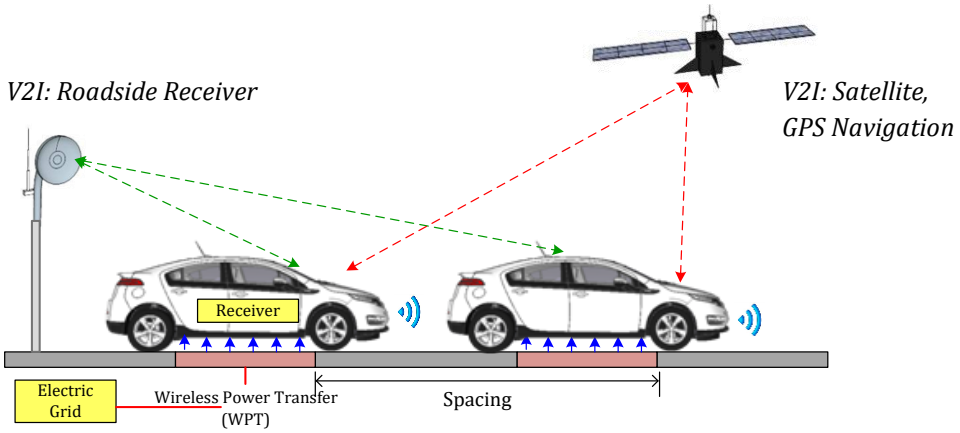

a) Configuration of AET system (*pictures from Google SketchUp)*

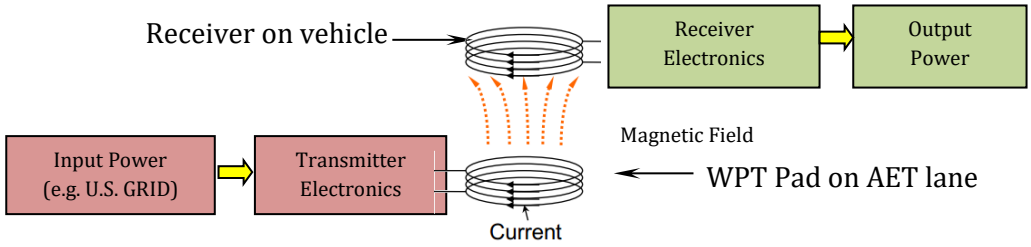

b) Wireless power transfer (*Adapted from Energy Dynamic Lab, USU*)

Figure 1 Configuration of AET system and schematic of wireless energy transfer

Further, it will be useful to define a number of terms used in this evaluation framework.

A Vehicle is an entity operating within an AET environment. An entity must be able to meet performance standards with respect to longitudinal maneuvers (acceleration and deceleration), lateral maneuvers, and communications (i.e., V2V and V2I). Three types of vehicles within an AET environment are classified by its role: i) *Singleton*: refers to the role of a vehicle operating outside of a platoon, ii) *Leader*: refers to the role of a vehicle in the front position of a platoon, and iii) *Follower*: refers to the role of a vehicle following a leader of a platoon. Figure 2a shows the three types of vehicles (i.e., singleton, followers and leader) in AET.

A Platoon is a grouping of vehicles traveling together and interacting in a cooperative manner to maintain a balance between objectives to maximize safety, system capacity, and individual travel needs (called *Steady State*). The maximum number of vehicles in the platoon (n) is governed by rules depending on the speed management, gap acceptance, platoon following and itinerary management.

Intra-Platoon following distance is the minimum distance determined based on the ability for the following vehicle to sense, interpret, command, and implement an emergency braking maneuver to avoid a collision with the leading vehicle. The limits to intra-platoon distance are governed by safety and aerodynamic advantages.

Inter-Platoon following distance is the minimum distance determined based on the ability for the following platoon to execute an emergency braking maneuver to avoid overrunning a platoon. It is also determined based on the headway associated with the minimum capacity advantage over a conventional freeway. Figure 2b depicts the state of platooning, intra- and inter-platoon distances.

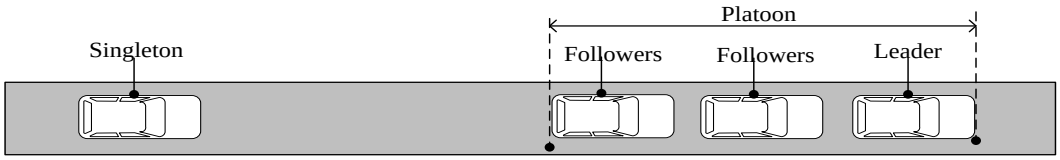

a) Leader, followers and singleton

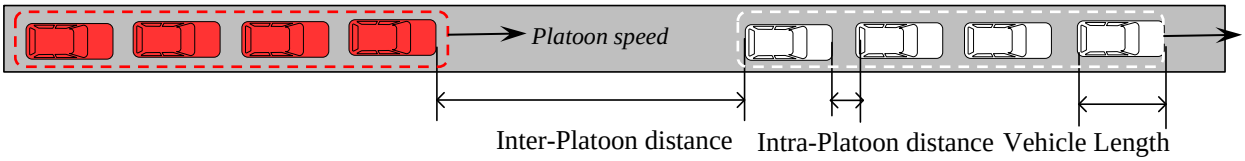

b) State of platooning (steady state)

Figure 2 Vehicle movements in AET system

3. AET evaluation framework

Figure 3 depicts the overall AET evaluation framework. The core component for the AET evaluation framework is the development of AET control logic, including car following and lane changing behavior of the singleton, leader and followers. The merging and diverging behavior of the singleton entering and exiting the platoon are also modeled to replicate the circumstance that a singleton desires to enter or exit the moving platoon. Note that we have modified the well-known Gipps car following model (Gipps, 1981) and use a simple stretch network to replicate the singleton car following and lane changing in AET lane. The interaction process from the singleton to platoon forming in the steady state has been modeled and tested in the microsimulation software, PARAMICS and its API. The parameters of the proposed model were calibrated to ensure the reasonableness of the movement in the AET lane. To validate the proposed model, the simulated results are compared against the analytical results derived in section 3.1. The vehicle profiles, including its position, speed, accelerate or decelerate, are recorded and further used for the evaluation framework. In our study, the evaluation focuses on three measures of effectiveness (MOEs) including: i) system capacity, ii) energy savings, and iii) environmental emission reduction. Note that for the environmental emission reduction, we adopted CMEM plug-in model in Paramics to evaluate the gas emission. Details of the evaluation framework are described as follows:

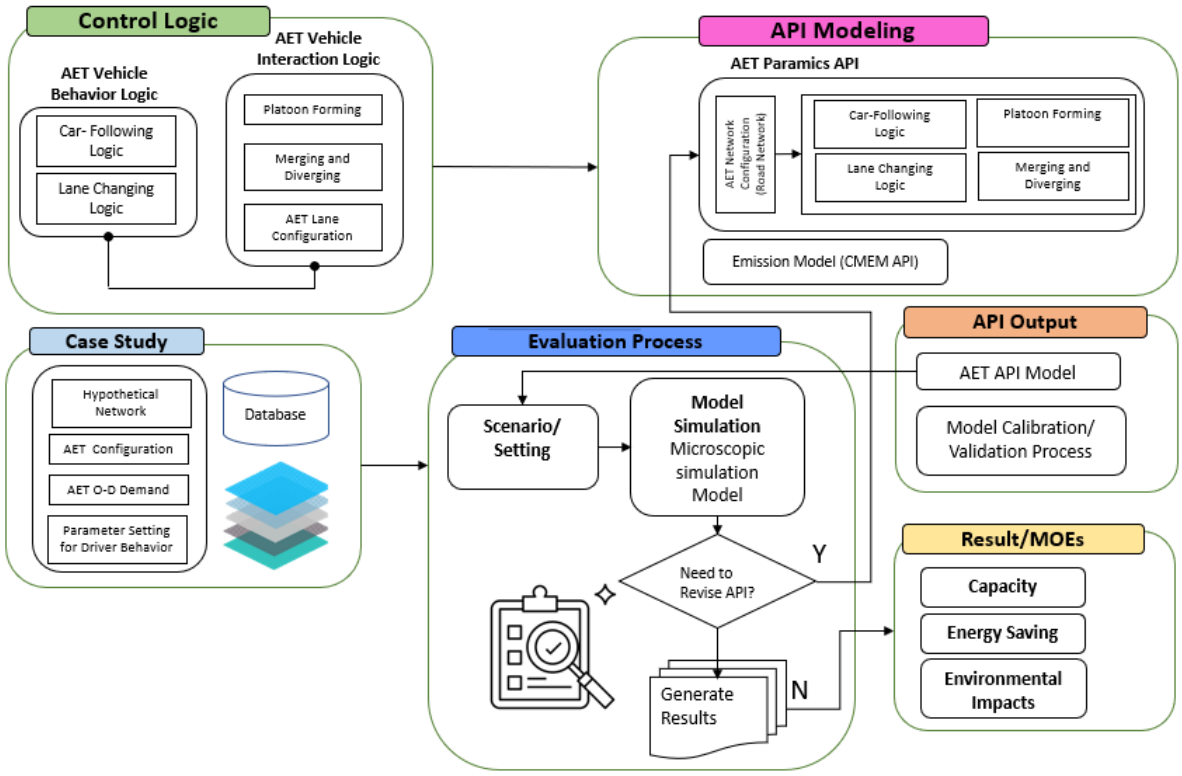

Figure 3 AET evaluation framework

3.1 System Capacity

Capacity is one of the potential benefits of platooning in an AET environment. According to the Highway Capacity Manual (TRB, 2016), the average flow rate in a multiple-lane highway at a speed limit 75 mph (about 120 kph) is about 1,800-2,200 veh/hr/lane and the highest record was just about 2,400 veh/hr/lane (or 45 pc/mi/lane). It represents a level of service (LOS) E for the highway segment. However, because of the advantage of automated control that eliminates the human factors of driving awareness, reaction time, and gap acceptance, the AET system is expected to achieve greater capacity if the traffic can be organized into platoons. According to past research and experiments of Automated Highway System (AHS) (Johnston and Ceerla, 1993), automated highways are expected to achieve at least *2.5 times* the capacity of a typical freeway lane (i.e., 2.5x2400= 6,000 veh/hr/lane). The feasible number of cars in the platoon can increase up to 20 vehicles per platoon. In addition, Horowitz and Varaiya (2000) stated that platooning decreases the mean inter-vehicle distance to achieve a capacity of up to 8,000 vehicles per hour per lane, as compared with the capacity of 2,000 veh/hr/lane in today's highways with manual-control. For AHS, capacity gains can likely be realized only through separate dedicated automated lanes (TRB, 1998). Considering these facts, we attempt to analyze the capacity of the AET system by using the fundamental relationship of traffic flow theory. Speed (u) in meter/min, density (k) in veh/meter, and flow (q) in veh/min are all related as shown in Eq. 1 below.

$$q = u \cdot k(s) \tag{1}$$

Note that the density is stated in the function of space headway, denoted as s. Density and space headway are also related as shown in Eq. 2. Typically, density is estimated from average space headway ($\bar{s}$):

$$k = \frac{1}{\bar{s}} = \frac{Z \cdot n}{\sum_i s_i} \quad (2)$$

where n is a constant size of platoon (veh) in the steady state, and Z is the number of platoons. Let us consider the steady state in Figure 2b, space headway of each platoon is the summation of vehicle lengths, intra-, and inter-platoon distances, as shown in Eq. 3 below:

$$s_i = nl_v + (n-1)h_{iv} + h_{ip}; h_{ip} \geq h_{iv} \quad (3)$$

where l_v is vehicle length (meters), h_{iv} is intra-platoon distances (meters), and h_{ip} is inter-platoon distances (meters). Assuming deterministic headway values in the steady state, density (veh/meter) can be written as shown in Eq. 4. Capacity (C), as the maximum flow that an AET system can accommodate, $C = q_{max}$, is shown in Eq. 5.

$$k = \frac{Z \cdot n}{Z[nl_v + (n-1)h_{iv} + h_{ip}]} = \frac{n}{nl_v + (n-1)h_{iv} + h_{ip}} \quad (4)$$

$$C = q_{max} = \frac{un}{nl_v + (n-1)h_{iv} + h_{ip}} \quad (5)$$

Consider when the number of vehicles in a platoon becomes larger, the theoretical capacity equals:

$$C = \lim_{n\to\infty} \frac{un}{nl_v + (n-1)h_{iv} + h_{ip}} = \lim_{n\to\infty} \frac{u}{l_v + h_{iv} + \frac{h_{ip}}{n}} = \frac{u}{l_v + h_{iv}} \quad (6)$$

Note that the AET capacity in Eq. 5 is similar to the capacity of AHS introduced by Varaiya (1993) and Eq. 6 is similar to *Rothery's equation* (Rothery, 1992) (i.e., $C = 1000V/S$, unit of C (veh/hr), V is speed (km/hr), S is average spacing bumper to bumper (meter); $S = l_v + h_{iv}$) which estimates capacity based on speed, vehicle length and intra-platoon distance. It is also important to note that platooning in AET succeeds by allowing a smaller intra-platoon headway (h_{iv}) than would normally be considered safe, and relies on the coordinated braking concept (Kanaris, 2010). The coordinated braking concept is based on the concept of maximizing capacity by carefully coordinating the timing and degree of braking among the vehicles participating in a platoon entity. In this paper, we assume AET performs in a perfect coordination among vehicles in order to maximize safety in the system. Our future research will try to relax this assumption and incorporate more factors that may affect the system safety (e.g., communication delay, packet delay and loss due to collisions or malicious attack). Note that the close following of vehicles are not practical outside an automated system, as human drivers lack ability to follow its predecessor very closely (as in only one meter apart), as well as, ability to react fast enough with such close spacing. It is also important to note that we consider AET with an exclusive lane consisting of mainline, entrance, and exit. The vehicles must enter or exit the AET system using check-in and check-out area. Under such conditions, the system capacity in this analysis is equivalent to *lane capacity*.

3.2 Energy Savings

The power supplied for AET vehicles (i.e., pure EVs, hybrid electric vehicles (HEVs)) generally comes from two major sources: i) its batteries, and ii) the WPT pads that are embedded along the AET lanes (as shown in Figure 1b). WPT is a method of delivering power to a device over an air gap - no physical contact is required. The Electric Vehicle and Roadway (EVR) research facility and test track at Utah State University have demonstrated the WPT technology for an electric bus with peak power of 25 kW at its

Electric Vehicle and Roadway test track in 2016 (Liu and Song, 2017). The power is transmitted via an air gap to the receiver installed underneath the vehicle and stored to the battery cells, which are typically assembled as the packs. Rechargeable lithium-ion (Li-ion) batteries are the most promising technology for EVs, HEVs, because it has: high power density to deliver the current needed for demanding driving conditions, high energy density for storing the needed energy for extended all-electric range, and wide range of State of Charge (SOC*) while maintaining a long cycle life (National Research Council, 2010).

In our framework, we consider the energy saving potential of EVs in an AET system compared with the conventional internal combustion engine (ICE) vehicles. Typically, tractive force (F_{tract}) in Newton (N) is used to propel a vehicle (for either EV or ICE) and overcomes certain resistance forces consists of inertial ($F_{inertial}$), rolling ($F_{rolling}$), aerodynamic (F_{aero}), grading (F_{grade}) forces as shown in Eq. 7 and Eq. 8. The schematic of the resistance forces is also depicted as shown in Figure 4a.

$$F_{tract} = F_{inertia} + F_{grade} + F_{rolling} + F_{aero} \tag{7}$$

$$F_{tract} = ma + mg\,sin(\theta) + c_{rr}mg + \frac{1}{2}\rho C_D A_f u^2 \tag{8}$$

where m is the total mass of vehicle (kg), a is acceleration (m/s^2), g is the acceleration of gravity ~9.81 m/s^2, θ is the degree of inclination, c_{rr} is the rolling resistance coefficient, ρ is density of air (kg/m^3), C_D is the air drag coefficient, A_f is the frontal area of a vehicle (m^2), and again u is the vehicle speed (m/s). The coefficients c_{rr}, C_D, and A_f can be simply obtained from the vehicle specifications published by the manufacturers. Note that the aerodynamic resistance is decreased in an AET environment (steady state) because of the drafting effect created by vehicles traveling at close spacing.

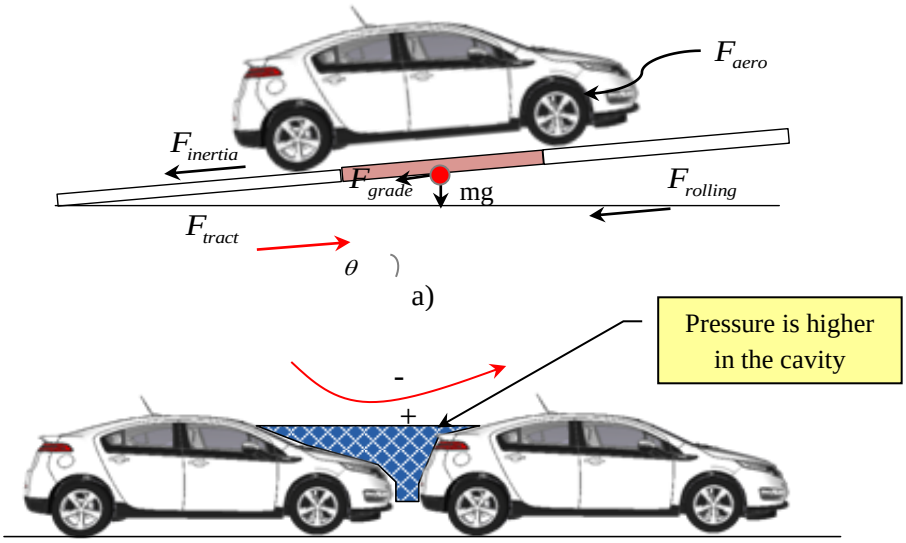

b) (adapted from Browand *et at.* (1996))

Figure 4 The schematic of resistance forces and aerodynamic benefits from closely following vehicles

* State of Charge (SOC): an expression of the present battery capacity as a percentage of maximum capacity.

Comprehensive experiments of close-following vehicles (in wind tunnel) conducted by Browand *et at.* (1996) revealed that there is an aerodynamic advantage associated with closely following vehicles. Figure 4b depicts the situation when two vehicles are sufficiently closed to each other to generate the aerodynamic advantage to decrease the drag of the front vehicle and increase the drag of the following vehicles. In this study, we just simply adopt the drag coefficients (C_D) for different number of vehicles in a platoon and spacing from the above study.

The power required to overcome the tractive forces (P_{tract}) in kN · m/s or kWatt is simply computed from the product of tractive force and speed as shown in Eq. 9. Hence, the total energy required for the vehicle depends on the power and the total travel time (Δt) (hour) used by an EV. The total energy (kW · h) is expressed in Eq. 10.

$$P_{tract} = F_{tract} \cdot u = c_{rr} mgu + \frac{1}{2}\rho C_D A_f u^3 + mau + mgu\, sin(\theta) \tag{9}$$

$$E_{tract} = P_{tract} \cdot \Delta t \tag{10}$$

Therefore, to compute the total energy used for each vehicle, we have to prepare the vehicle activity profile including its position, speed, and acceleration. The energy usage can be classified into three levels:

- *Individual level*: energy usage per vehicle (E_{tract}). E_{tract} can vary by vehicle weight, position and role (e.g., singleton, leader or follower which directly affects the activity profile), acceleration, deceleration rates, and travel time.
- *Platoon level*: energy usage per platoon (E_p) is a summation of energy use for all vehicles in a steady-state platoon. The level of energy usage per platoon depends on platoon size, platoon speed, and platoon travel time.
- *System level*: system-wide energy usage (E_{total}) is computed by summing the energy use for all vehicles in an AET system. Alternatively, E_{total} can be approximately estimated by summing the energy used by all platoons (i.e., $E_{total} = \sum_{P \in Z} E_P$).

3.3 Emission Reduction

Conventional ICE vehicles are responsible for various emissions, including CO_2, CO, NO_x, HC, and so on. The EV, on the other hand, produces little or no pollution directly to the transportation system. Typically, pure EV or battery electric vehicles (BEVs) have no tailpipe emissions, and are not reliant on fossil fuels. Though EVs produce no tailpipe CO_2 emission, they still have emissions produced by the source of electric power, such as a power plant (or called the *well-to-wheel emissions*). To calculate CO_2 emission of *well-to-wheel*, the grid average CO_2 emission intensity (gram CO_2 /kWh) of power generation mix (also known as the average emission factor, AEF) is an important factor. The CO_2 emission intensity can vary considerably depending on the power sources (i.e., coal, crude oil, biodiesel, etc.). Sovacool (2008) estimated a mean value of CO_2 emission intensity of power plants by averaging the global results, and some of these findings are summarized in Table 1.

This study investigates the CO_2 emissions of EVs compared to those from similar ICE-based vehicles. In order to achieve this, we adopt the Comprehensive Modal Emission Model (CMEM) (Barth et al., 2000) developed by the Center for Environmental Research Technology (CERT) from the University of California at Riverside. CMEM is based upon vehicle technology in 40 categories. The vehicles used in the CMEM database are representative of a wide range of vehicles, from the normal vehicle without catalysts to the super ultra-low emission/partial zero-emission vehicle.

Table 1 Grid-average CO_2 emission intensity of power plant

Technology	CO_2 emission intensity (gram CO_2 /kWh)
Wind	10
Biogas	11
Solar Power	13
Nuclear	66
Natural Gas	443
Diesel	778
Coal	960

Source: Sovacool (2008)

The second-by-second vehicle tailpipe emissions are modeled as the product of two components: fuel rate (FR) and engine-out emission indices. The model estimates second-by-second emissions as well as fuel consumption in various ICE vehicle operating conditions (i.e., idle, cruise, acceleration and deceleration) based on power demand. Tailpipe emissions for ICE are calculated using FR, engine-out emission indices (gram emissions/gram fuel) and time dependent catalyst pass fraction (CPF) as follows.

$$Tailpipe\ emissions = FR \cdot CPF \tag{11}$$

4. Model development and evaluation

4.1 Developing AET in the Simulation Model

The key to the proposed evaluation framework is to develop a model of AET system and evaluate its system performance in the microscopic simulation paradigm. The challenge is to develop a traffic simulation model that can reproduce the ideal capacity in the AET environment, which could be much greater than the current practical highway capacity. This study adopts Paramics, a microscopic simulation platform to mimic the proposed system. Paramics is a commercial software package, which is capable of simulating various Intelligent Transportation System (ITS) strategies, high occupancy vehicle (HOV) lanes, high occupancy and toll (HOT) lanes, etc. A simple schematic of an AET network consists of two links connecting between an origin and a destination (O-D). The first link connected to the origin is used for platoon forming, and we place the detectors on the other link in order to measure the capacity of the system. To simulate the platoon forming in AET, we developed the application programming interface (API) functions by overriding speed, acceleration, and deceleration models in Paramics. Paramics Programmer allows users to augment the core Paramics simulation with new functions, driver behaviors and practical features with API. Researchers can override or replace sections of the core Paramics simulation with their own behavioral models, such as car following, lane changing, and route choice models. The following subsections explain two major AET models: i) platoon forming and ii) lane changing models.

i) Platoon Forming Model

The AET platoon forming was developed from the car following model. A series of investigations on this model were explored. The following groups are the car following models classified based on the concept behind the model including i) Psychophysical model (Chandler, 1958; generalized GM model researcher by Kometani and Sasaki 1959) ii) Safe distance model (Gipps model, 1981, Krauss model, 1997, Intelligent Driver Model (IDM) by Treiber et al., 2000), iii) Action point model (Leutzbach model, 1988),

iv) Cellular automata model (Nagel and Schrekenberg, 1992), v) Optimum velocity model (Bando et al., 1995), and vi) Trajectory based model (Newell model, 2002). Gipps (1981) proposed a safe distance model that contains a number of parameters, which can be calibrated for different behavior features of drivers including acceleration, deceleration and maximum or desired speed, and so on. The model is widely preferred for simulation purposes, thus, we modified Gipps model for the AET system. For a vehicle (*n*), the maximum speed required to accelerate during a time period (*t*, *t*+*T*) is given by:

$$V_a(n,t+T) = V(n,t) + 2.5 \cdot a(n) \cdot T\left(1 - \frac{V(n,t)}{\bar{V}(n)}\right) \cdot \sqrt{0.025 + \frac{V(n,t)}{\bar{V}(n)}} \tag{12}$$

The speed of the decelerating vehicle (*n*) when approaching a lead vehicle (*n*-1) during time interval (*t*, *t*+*T*) is given by:

$$V_b(n,t+T) = d(n) \cdot T + \sqrt{d(n)^2 \cdot T^2 - d(n)\left[2 \cdot \{x(n-1,t) - s(n-1) - x(n,t)\} - v(n,t) \cdot T - \frac{v(n-1,t)^2}{d'(n-1)}\right]} \tag{13}$$

where $V(n,t)$ is the speed of vehicle *n* at time *t*; $\bar{V}(n)$ is the desired speed of the vehicle *n* for current; $a(n)$ is the maximum acceleration for vehicle *n*; T is the reaction time; $d(n)$ is the maximum deceleration desired by vehicle *n*; $x(n,t)$ is the position of vehicle *n* at time *t*; $x(n-1,t)$ is the position of preceding vehicle *n-1* at time *t*; $s(n-1)$ is the effective length of vehicle *n-1*, $d'(n-1)$ is an estimation of vehicle *n-1* desired deceleration.

The parameters of 2.5 and 0.025 in Eq. 12 are arbitrarily chosen as originally introduced by the model's developer, while acceleration, maximum desired speed, time interval, deceleration or braking rate can be modified according to the AET control maneuvers. The parameter *T* corresponds to the reaction time, which is assumed to be equal for all drivers in the AET system. Note that in the AET system we assume the reaction time for each vehicle is decided and fully controlled by the AET control system. In any case, the definitive speed for vehicle *n* during time interval (*t*, *t*+*T*) is the minimum of those previously defined speeds:

$$V(n,t+T) = Min\left(V_a(n,t+T), V_b(n,t+T)\right) \tag{14}$$

Moreover, for the AET model, the speed of vehicle in the proposed system is fully controlled. The important key for modeling the AET system, thus, is to adjust the parameters (i.e., vehicle position $x(n,t)$ and desired deceleration, *d'(n-1)*) in order to maintain the desired intra-platoon and inter-platoon distances, and hence ultimately achieve the optimal system capacity. Let us consider the optimal desired deceleration of lead vehicle *d'(n-1)* with a desired gap distance (*G*), where $G \geq h_{iv}$, can be expressed as:

$$\bar{d}'(n-1) = \frac{d(n) \cdot v(n-1,t)^2}{\left(v(n-1,t) - d(n) \cdot T\right)^2 - d(n)^2 \cdot T^2 + 2 \cdot d(n) \cdot G - d(n) \cdot V(n,t) \cdot T} \tag{15}$$

The desired deceleration *d'(n-1)* in Eq. (15) indicates that there is no speed change when the following vehicle $x(n,t)$ approaches the lead vehicle with the desired gap distance. Using Eq. (15), we can rewrite Eq. (13) as follows:

$$V_b(n,t+T) = d(n)\cdot T + \sqrt{d(n)^2\cdot T^2 - d(n)\left[2\cdot\{dis(n-1,t)\} - V(n,t)\cdot T - \frac{v(n-1,t)^2}{\bar{d}'(n-1)}\right]} \quad (16)$$

where $dis(n-1,t) = x(n-1,t) - s(n-1) - x(n,t)$. In order to implement the above car-following concept, a pseudo code in Paramics API for the platoon forming logic is given in Appendix A.

ii) AET Merging and Diverging Models

The AET merging model is an operational model for an AET vehicle to access the AET lane after the check-in procedure (for check-in procedure or entrance algorithm, see Heaslip *et al*, 2011). The major components of AET consists of an exclusive mainline, entrance and exit. The major difference between AET and conventional highway is that the vehicle that desire to use AET lane must enter or exit using the check-in and check-out areas located adjacent to the entrance and exit areas. The hypothetical AET system can automatically manage these vehicles using a controller (or centralized decision system) that decide how and when to release the vehicle from the entrance ramp and the mainline and diverge the vehicle from platoon to exit and check-out areas. The merging strategy that considers the *acceptable safe gap distance* for a vehicle or group of vehicles queued on the on-ramp to safely merge to the mainline traffic stream was developed. The acceptable safe gap distance is defined as the distance of inter-or intra-platoon space headway that allows vehicle(s) to safely merge into the mainline traffic. The procedure for measuring this gap and releasing vehicles queued on the entrance ramp to merge into mainline traffic resembles that of an advanced ramp metering system. Typically, ramp metering techniques can be divided into three categories: pre-timed, traffic-responsive, and predictive. In the traffic-responsive approach, detectors and computers are utilized to determine mainline flow and ramp demand in the immediate vicinity of the ramp, and an appropriate metering rate is set. The merging model consists of three consequent procedures: i) determination of the number of vehicles on the AET mainline, ii) releasing the vehicle(s), and ii) lane changing from transitional lane to AET lane. Figure 5a shows such a merging procedure.

The diverging model is another operational model for diverging an AET vehicle from the AET lane to the off ramp and check-out area. To implement this model, the typical lane changing model is implemented. When the vehicles desire to exit the AET system, they need to start to perform the lane changing maneuver using the transitional lanes beside the AET lane. Figure 5b shows such a diverging procedure. For more details, pseudo codes in Paramics API for the merging and diverging are given in Appendix A. In this study, we assume that the merging vehicles are released from the ramp to join the tail of the platoon as depicted in Figure 5a based on the availability of gap distances and approaching platoon size. With this assumption, the platoon split and deceleration maneuver are not required. Note that the platoon split in the proposed system may further complicate the platoon operation regarding the safety issue. This assumption is beneficial for the AET operation as it provides a simple way to manage the merging vehicles and platoon on the mainline. The number of vehicles releasing to the mainline is adaptive as it uses a similar ramp metering concept. However, the drawback of the proposed operation is that it may not provide us the maximum mainline capacity and efficient ramp metering as the merging vehicles need to wait for the availability of gap distances and the number of vehicles in the platoon must not exceed the maximum platoon size. In case of congested conditions (e.g., during peak period), the merging vehicle may need to wait longer for the availability of adequate gaps, and thus we may need to modify the merging strategy to accommodate this situation.

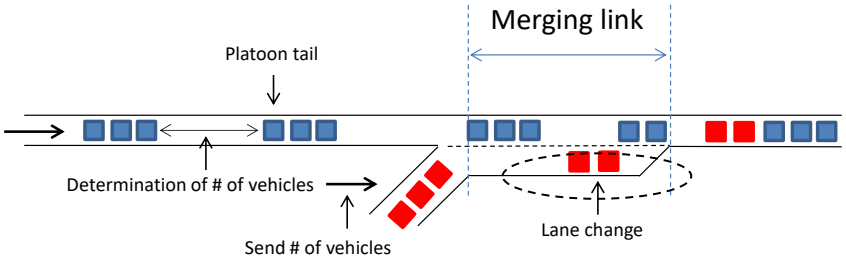

a) Merging procedure

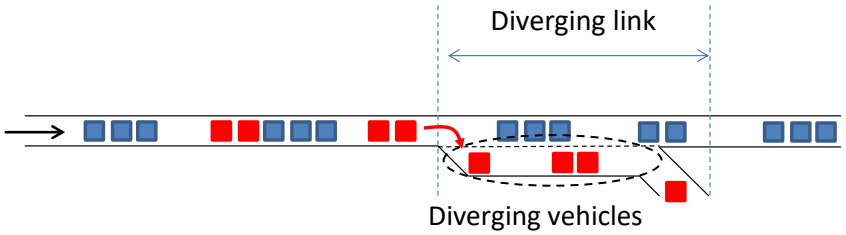

b) Diverging procedure

Figure 5 Merging and diverging procedures in AET

The integrated hypothetical AET system that has diverging and merging system is modeled as shown in Figure 6. As can be seen, the AET system has the check-in and check-out areas located adjacent to the on- and off-ramp areas. The AET control system gathers traffic information from mainline including: number of approaching platoons, platoon size, gap distances and the number of vehicles desired to diverge from the AET mainline and their speed from the upstream at the diverging area. On the ramp, the number of vehicles checked-in and number of vehicles releasing to join the moving platoon on the mainline are computed and decided from AET controller. The simulation model that accommodates the AET merging and diverging was set up and evaluated.

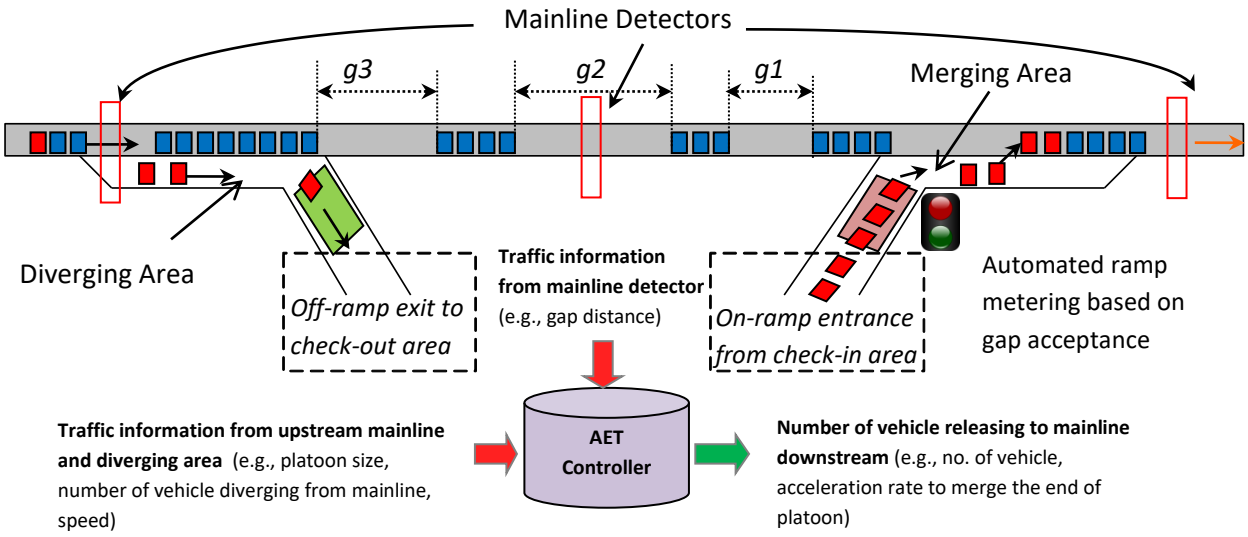

Figure 6 Hypothetical AET System with Diverging and Merging

Figure 7a depicts the traffic data obtained from the detector located at the upstream, downstream and ramp (waiting area and transitional area). The counting period at the detector is at every 5 minutes. As can been observed, the number of vehicles at the mainline is approximately 700 vehicles per 5 minutes (about 8,400 vph). Similarly, the traffic flow after the merging and diverging are slightly impacted due to these effects and they outperform the conventional highways.

However, the more realistic impact of the mainline shockwave should be investigated in the future. The traffic flows at the transitional lane or acceleration lane and the mainline are similar, implying the releasing logic is efficient for the merging process without disturbing the mainline traffic. The synchronization between merging vehicles to join the tail of the platoon is the key for maintaining the effective operation of the mainline. It should be noted that here we build the transitional lane that is sufficiently long to facilitate the lane changing of merging vehicles. In this case, the minimum length of the acceleration lane for merging vehicles to the mainline is about 300 meters. The distance is on the average length according to the recommendation by AASHTO guidelines. Figure 7b and Figure 7c show the accumulative counts at those locations.

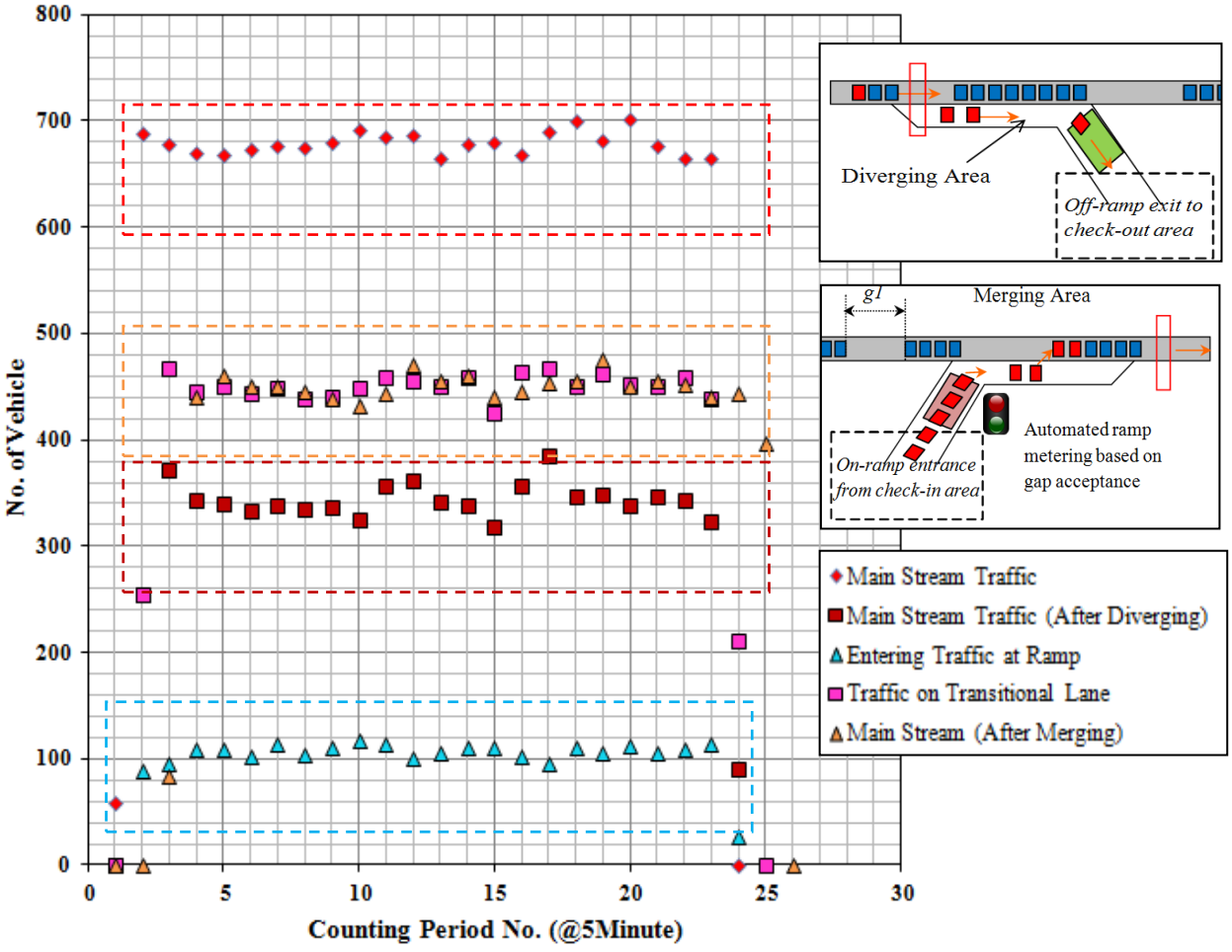

a) Detecting Data at Mainline, Diverging and Merging Locations

Figure 7 Simulated detector data at mainline, diverging and merging locations

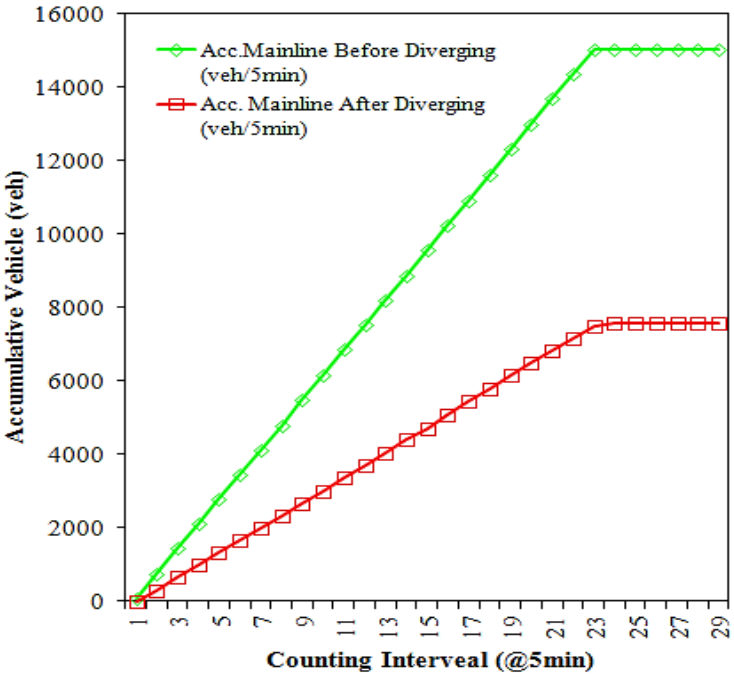

b) Accumulative volume before diverging

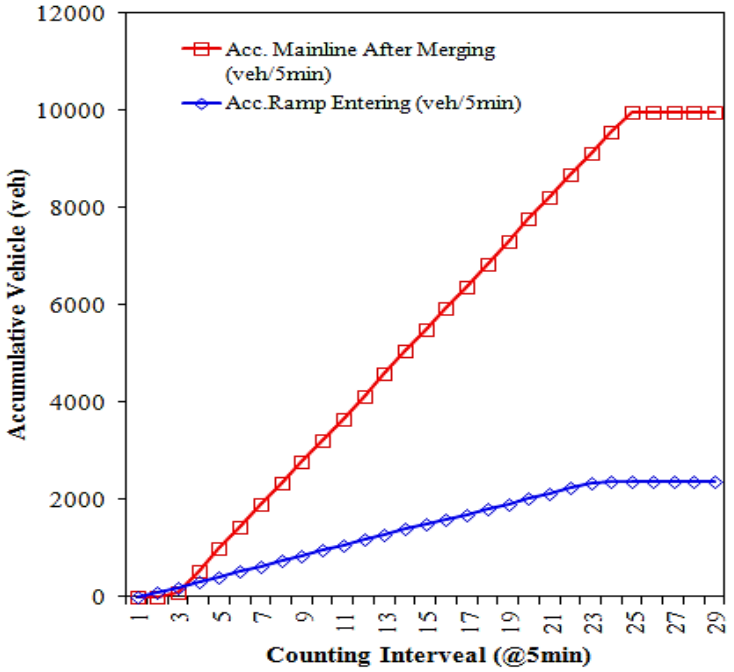

c) Accumulative volume after merging

Figure 7 (Cont.) Simulated detector data at mainline, diverging and merging locations

4.2 Capacity Analysis

As defined previously, the capacity of AET can be obtained from the simulation model. In order to estimate capacity at different AET operation conditions, different numbers of vehicles in a platoon or platoon sizes are simulated. Table 2 shows the results obtained from the proposed model compared with the calculated capacity for different platoon sizes. Note that the calculated results in this subsection were computed based on the analytical formulations in Section 3. The speed limit, vehicle length, intra- and inter-platoon distances were set to be 120 kph (75 mph), 5 meters, 1 meter and 30 meters, respectively. In this preliminary experiment, we assume the homogeneity of traffic demand (i.e., one vehicle type) that travels directly from origin to destination. The capacity of manual control was calculated based on the Highway Capacity Manual. As can be seen, the results of simulated capacity agree with the calculated ones. We can observe that capacity of 1-veh platoon (the minimum case) indicates the capacity of 3,428 veh/hr, or about 50% higher than the manual control. A proportional increase of flow rates relative to the platoon sizes is depicted in Figure 8. In the case of an infinite platoon (h_{iv}=h_{ip}=1 meter), capacity of the maximum case can reach to 20,000 veh/hr., which is far beyond today's highway capacity. However, in practice, the maximum capacity is very difficult to be obtained because of several reasons. They are, for example, several perturbations of traffic due to merging and diverging vehicles as mentioned in the previous section. The merging vehicles can induce high perturbations for AET system as the mainline platoons and/or singletons are forced to decelerate in order to avoid a collision with the merging vehicles. The non-homogeneity of traffic flows (i.e., short and long ranges) can potentially reduce the capacity as the short range vehicles need to change lane in order to exit the system, while the long range vehicles have to adjust to reform a platoon. Conducting a comprehensive AET operation that accounts for these situations would be necessary in our future research.

In addition, we assess the sensitivity of capacity at different intra- and inter- platoon distances with speed range between 80-120 kph or about 50-75 mph. Figure 9a depicts the results of system capacity when we fixed inter-platoon distance to 30 m. while Figure 9b depicts the one of fixed intra-platoon distance to 1 m. Figure 9b shows that the system capacity drops sharply when the intra-platoon distance is farther compared to the inter-platoon one. In other words, it implies that the system capacity is more sensitive to intra-platoon distance than the inter-platoon distance. Overall, the capacity analysis indicated that AET capacities of approximately 1.5-8 times higher than those of typical highway are possible for platoons of automated passenger vehicles. The synchronization between merging vehicles to join the tail of the platoon is important factor for AET for maintaining mainline AET lane capacity. However, limitations in the capacity analysis do exist, which should be addressed in the future: uniform and mixed vehicle type, mixed vehicle' braking performances, wireless communication performance between infrastructure and vehicles (V2I).

Table 2 Comparison between calculated and simulated capacity

Type of Control	Density		Calculated Capacity	Simulated Capacity	Previous Research
	(veh/km)	(veh/mile)	(veh/h)	(veh/h)	(veh/h)
Manual Control	28.00	45.00	2,250[†]	-	-
AET Control					
1-Veh Platoons	28.55	45.97	3,428	3,428	
5-Veh Platoons	84.69	136.38	10,169	10,169	
10-Veh Platoons	112.30	180.84	13,483	13,484	7,909 (AHS*)
15-Veh Platoons	125.96	202.83	15,126	15,124	8,007 (AHS*)
20-Veh Platoons	134.14	216.00	16,107	16,106	
25-Veh Platoons	139.58	224.77	16,759	16,760	
AET Maximum Case (Infinite Platoon)	166.57	268.22	20,000	20,000	

[†] *Based on HCM LOS E, Speed of 50 mph, *Free agent infrastructure managed platoons/ dry road surface ,max headway= 3m., min headway=7.1m.*

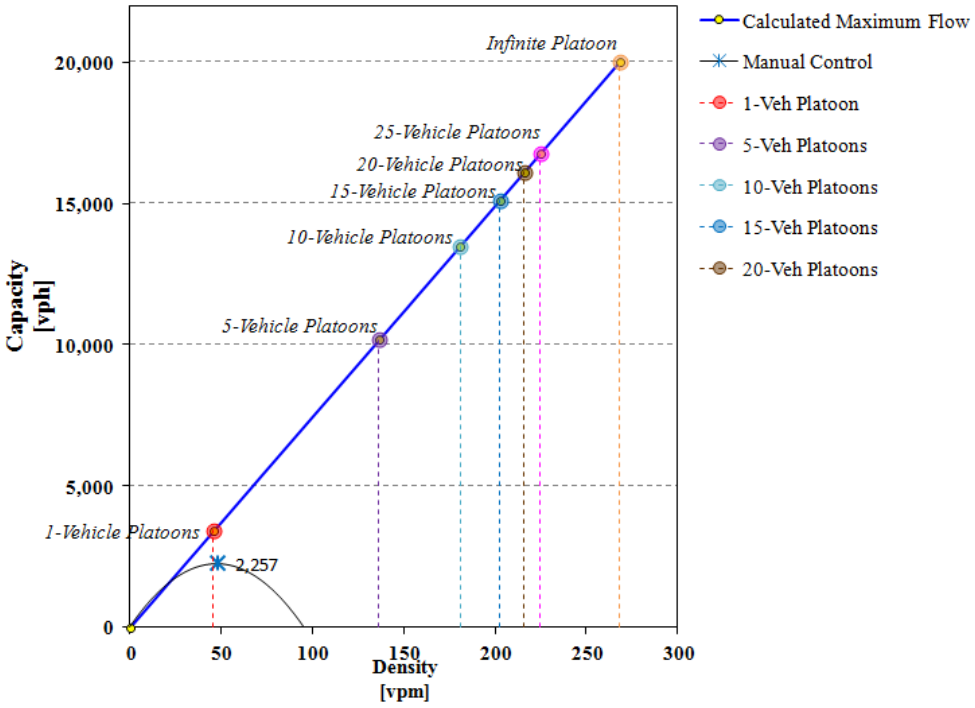

Figure 8 Capacity of a platoon under AET system (Simulated Cases)

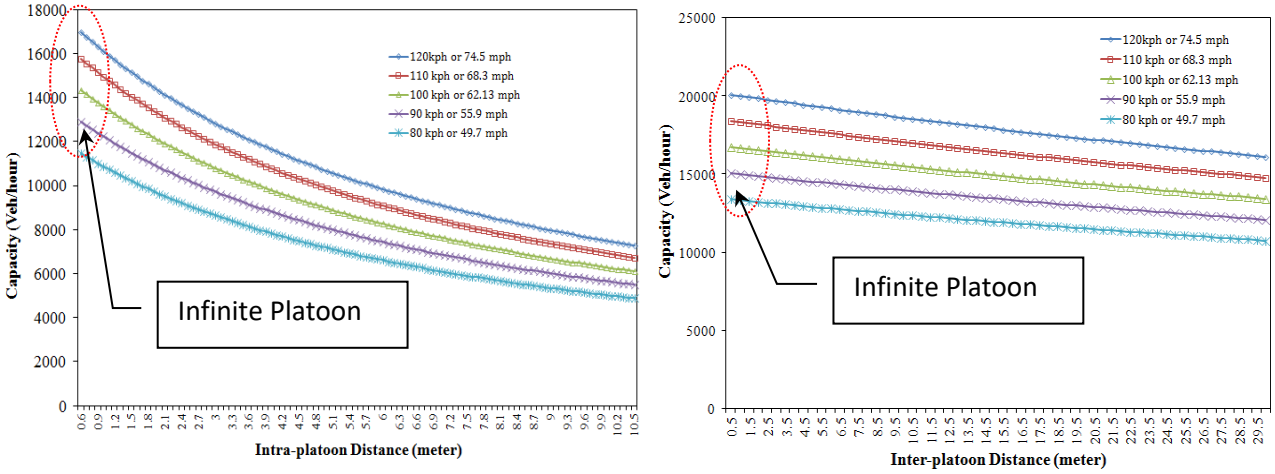

a) Intra-platoon distances ($h_{ip} = 30$) b) Inter-platoon distances ($h_{iv} = 1$)

Figure 9 Capacity of a platoon under AET system for different intra- and inter-platoon distances (20 vehicles per platoon)

4.3 Energy Analysis

4.3.1 Power Consumption

To calculate the power and energy needed to achieve the velocity and acceleration in AET system, the activity profiles of vehicles were collected from the simulation model. The manual control was also simulated using the same network in order to compare energy usage and emissions to the AET system. We adopted parameters of mean target headway and reaction time from the California ATMS Testbed (I-5 freeway) (Lee et al., 2001). In that case, a genetic algorithm technique was developed to calibrate headway and reaction time (i.e., headway = 0.615 seconds and reaction time = 0.415 seconds). In this study, we use the 2008 Toyota Camry, a mid-size sedan, in our experiment. According to the specifications, the mass of vehicle is 1,588 kg., the coefficient of drag (C_D) is 0.28, the frontal area is 2.7 m^2, and AET lane is on flat terrain (θ =0). The coefficient of rolling resistance (c_{rr}) for tires is assumed to be 0.01, and the density of air (ρ) is 1.2 kg/m^3. A 745-W constant load (about 1 horsepower) was added to account for the power needed for accessories such as air conditioner, heater, radio and lights. Recall that the aerodynamic resistance is decreased when vehicles form a platoon. The aerodynamic resistance reduction as a function of vehicles in a platoon and spacing (meter) was computed. Figure 10 depicts the aerodynamic resistance of vehicles in a platoon; here we demonstrate two average speeds: 120 kph or about 75 mph (in Figure 10a), and 105 kph or about 65 mph (in Figure 10b). Note that we convert speed from meter/min to kph in this analysis. As can be observed, at higher speed, more power is required to overcome the aerodynamic resistance. However, when the spacing between vehicles decreases, the reduction of aerodynamic resistance significantly decreases. Likewise, results also show the benefits of aerodynamic resistance reduction when the number of vehicles in a platoon increases. In AET, all vehicles in a platoon share this drag saving benefits, and consequently can reduce the overall tractive force and ultimately power, and energy usage.

The activity profiles of AET and manual control vehicles were then collected from the microsimulation models. Here we select the case of 10-vehicle platoon (speed 105 kph, $h_{iv} = 1\,\text{m}$, $h_{ip} = 30\,\text{m}$) for illustration. Figure 11 shows the sample activities of the leader (i.e., 1st vehicle), the 5th follower, and the 10th follower, respectively. Figure 11a depicts the speed profile of vehicles in an AET system. Under the cooperative control manner, AET vehicles are formed into a platoon (steady state) in a short amount of time compared to the Manual Control vehicles (in Figure 11b). The acceleration profile (in Figures 11c and 11d) shows fluctuations in accelerations of the 10th vehicle when it is a singleton. This is expected because AET attempts to adjust the acceleration/deceleration behaviors of the singleton in order to form a platoon in the AET link. The maximum deceleration rate for the 10th AET vehicle is about 4.5 m/s^2 (slightly higher than the comfortable deceleration rate of 3 m/s^2 (Chakroborty and Das, 2005)). However, there is very low fluctuation (almost zero) after the vehicle merges to a platoon. For the Manual Control vehicles, we can observe very high fluctuation in accelerations of the 5th, and the 10th follower. With all these results, we can calculate the power consumption profiles as in Figures 11e and 11f. For an AET system, the power consumption increases significantly at the earlier stage mainly due to the inertial forces required for platoon forming.

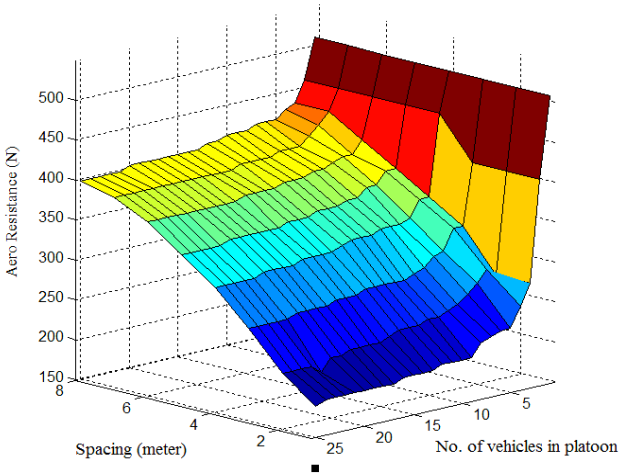

a) Speed 120 kph (75 mph)

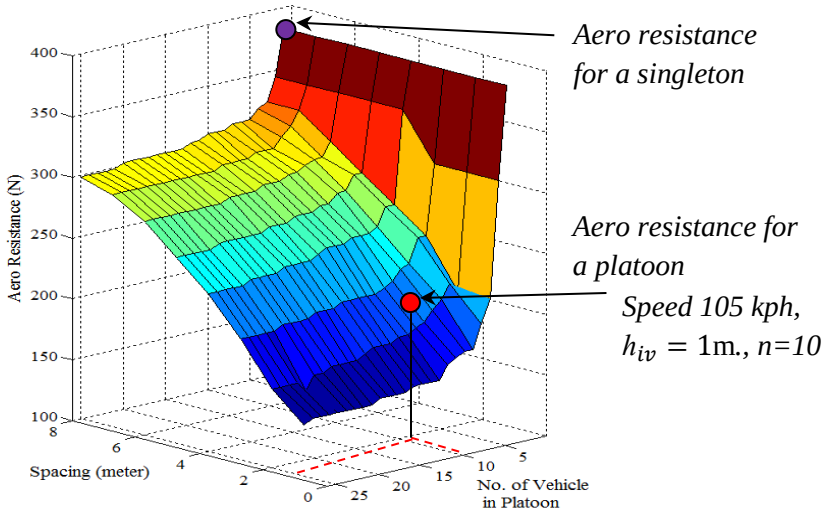

b) Speed 105 kph (65 mph)

Figure 10 Estimated reduction in aerodynamic resistance for a platoon

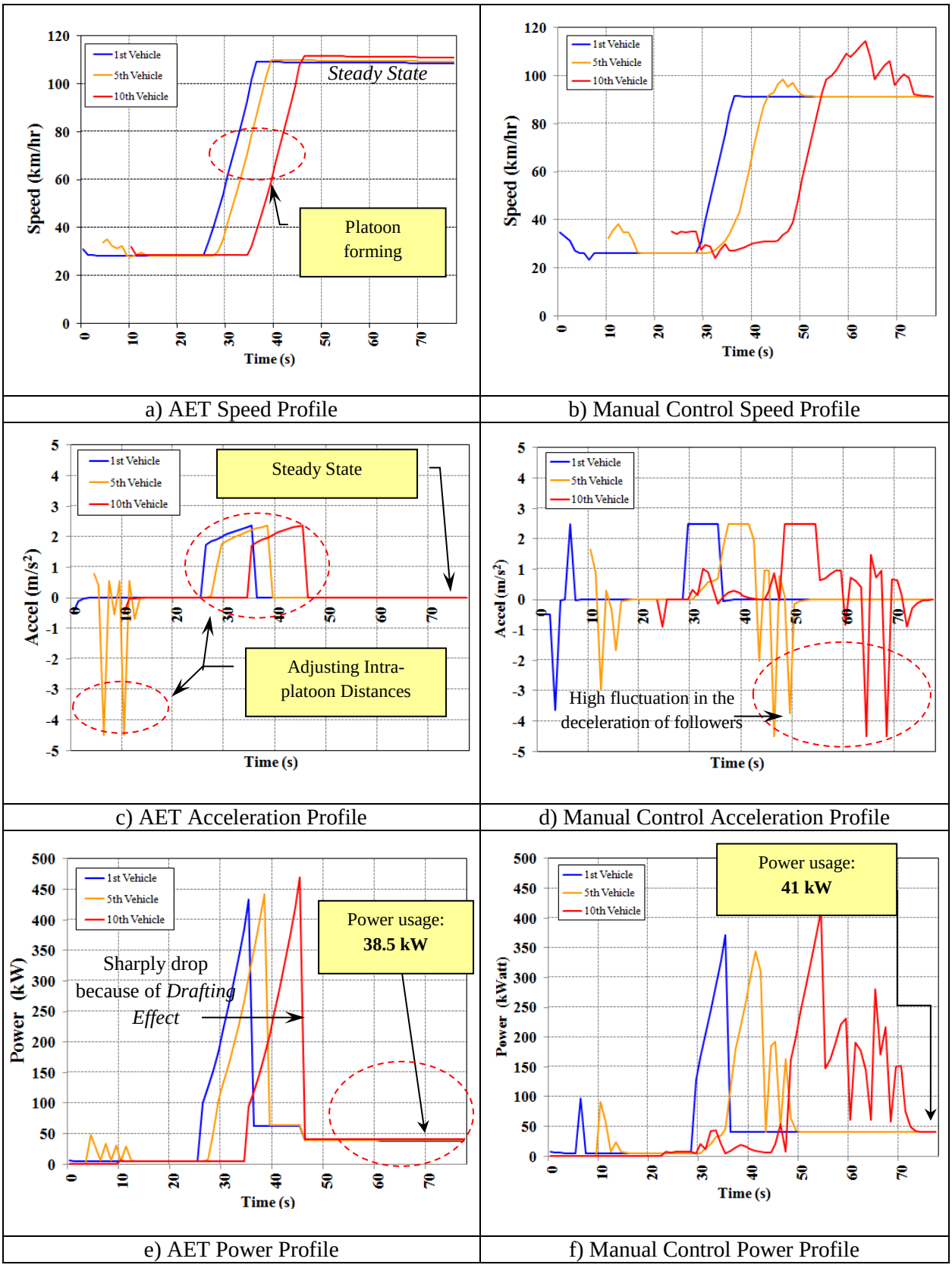

a) AET Speed Profile | b) Manual Control Speed Profile

c) AET Acceleration Profile | d) Manual Control Acceleration Profile

e) AET Power Profile | f) Manual Control Power Profile

Figure 11 Speed, acceleration, and power profiles for AET and Manual Control vehicles

The power consumption for AET drops significantly to about 38.5 kW due to the drafting effect (final F_{aero} ~198N, see Figures 11e and 11f). This number is slightly lower than the Manual Control one which consumes about 41 kW. The energy (kWh) is calculated using Eq. 10. Using these simulation results, the vehicle would use 0.35 kWh/km (about 0.56 kWh/mile). With the battery pack of 24 kWh storage capacity (e.g., used in Nissan Leaf), the driving range of AET is about 45 km. (about 28 miles) without recharging. However, this may not satisfy the higher range of travel (i.e., interstate trips, freight transportation), and thus emphasizing the importance of AET system in the future.

The cumulative distribution of energy was calculated to illustrate the amount of energy used during the platoon forming process under various speeds in Figure 12. As can be observed, during the platoon forming stage, AET requires large amount of energy for such movements and becomes lesser after all vehicles move at a cruising speed. Consequently, the system planners may use this information to estimate the energy needed for the AET system (via WPT).

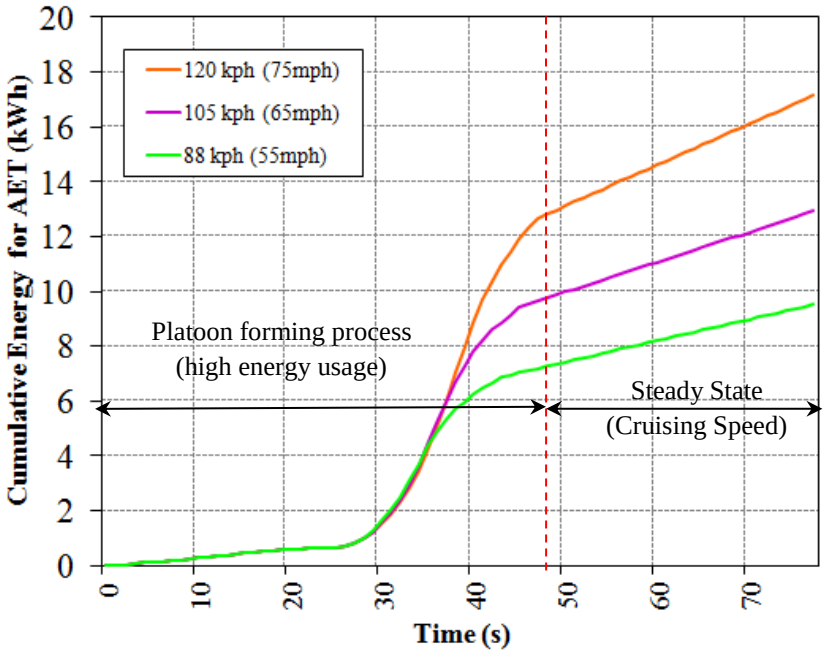

Figure 12 Accumulative energy usage per platoon at different speeds
(Platoon size=10, h_{iv} = 1m, h_{ip} = 30m.)

4.3.2 Wireless Power Transfer (WPT) for AET System

In this section, a preliminary analysis for energy consumption derived from the wireless power transfer (WPT) for the AET system was analyzed. The wireless power transfer from the magnetic resonance coupling antenna from the roadway to vehicle. Budhia et al. (2009) studied the in-motion wireless power transfer (IPT) for varying vehicle speeds. Figure 13a depicts the percentage of efficiency at different vehicle speeds from their study. The efficiency of WPT is decreasing significantly when the vehicle speed increases. The percent efficiency of the highway speed of 65 mph is approximately about 55%. This is the challenge for the AET system. The Energy Dynamics Lab at USU has proposed to develop an IPT system that has at least 90% efficiency at the operation speed of 75 mph at 40 kWh. Note that the air gap between pad underneath the vehicle and the antenna embedded on the roadway of the proposed system is about 10-15 inches. The air gap is the key factor for the future implementation to other types of vehicles, including bus and truck which usually require the larger air gaps than those of passenger cars. To assess the different IPT efficiencies in the AET system, we also use the simulated

results obtained from the previous section using commuting electric vehicle (EV) on the highway speed of 65 mph. Figure 13b shows the energy consumption of the AET vehicle with a full battery capacity of 24 kWh. As can be observed, the maximum range of vehicle with the battery only is about 42 miles. However, with a 55% efficiency for WPT, the maximum range of the same vehicle is extended to about 82 miles (about 2 times of battery only model). It also shows that the AET vehicle can travel along the AET lane without a need to stop for recharging with the WPT efficiency at least 90%. The result in this section highlights the importance of WPT in the AET system that could extend the travel distance and could be the key to overcome the range anxiety, which is the major barrier to large scale adoption of electric vehicles.

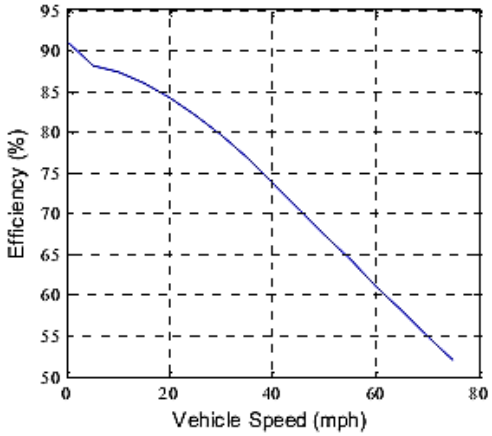

(adapted from Budhia et al., 2009)

a) WPT efficiency

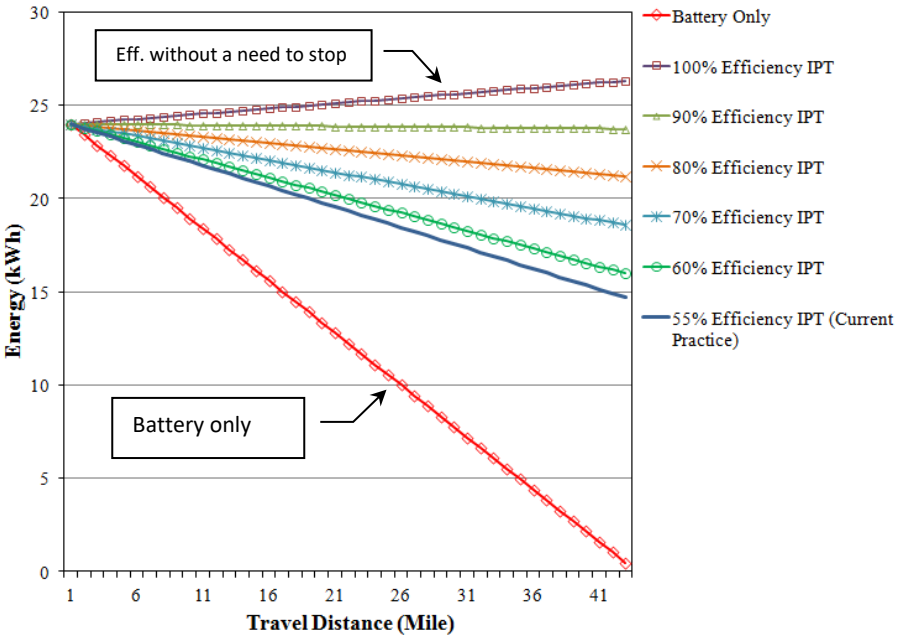

b) Energy consumption

Figure 13 AET system efficiency and its range

4.4 Emission Analysis

Electric vehicles in the AET system help improve air quality in the urban areas, specifically reduce direct emissions including greenhouse gases (GHGs), smog-forming pollutants, and Particulate Matter (PM) in the air. The emission analysis in our evaluation framework adopts the Comprehensive Modal Emission Model (CMEM) plug-in model in Paramics to generate the emission including tailpipe emissions of HC, NOx, CO2, and CO, while converting the energy consumption rates obtained from the previous analysis to *well-to-wheel* emissions. The emission model is directly connected to the AET simulation model by accessing to every individual vehicles' position, speed, and acceleration activities of both AET and other non-AET vehicles. The CMEM has been developed under the National Cooperative Highway Research Program NCHRP Project 25-11 as power-demand model based on a parameterized analytical representation of emissions production. These parameters related to various factors obtained from known vehicle manufacturers (e.g., vehicle mass, engine size, aerodynamic drag coefficient, etc.) are integrated in the model to compute the individual vehicle's emission. Note that the ICE vehicle emission rate is based on the super ultra-low emission vehicle/partial zero-emission vehicle (category 27 in CMEM equivalent to a 2008 Toyota Camry). Figure 14 depicts the tailpipe emissions of all four gases that computed from the simulated results. We estimate the total emission based on the total number of vehicles in the AET platoon (i.e., $h_{iv} =$ 1m, $h_{ip} = 30$m.). The speed is varying from 10 to 85 mph, which reproduce the total vehicles of 2,160-18,361 vph. As expected, the results indicate the amount of CO_2 increases significantly when the platoon speed increases and more throughput vehicles in the system. The trends of HC and NO_x are similar to CO_2, but not for CO, which slightly increases. The result implies a great benefit in terms of emission reduction when the vehicles join the AET system.

In the case of electricity, electric power plants produce emissions associated with the processing of the primary energy sources for their productions. The CO_2 emission rates (in gram) per platoon for a 10-vehicle platoon per km were summarized in Table 3 to demonstrate the results from different *well-to-wheel* emission that could be the energy sources for AET system. As can be observed, the emission rates are an important factor and this can significantly change the CO_2 intensity of a power generation. In the U.S. in 2018, natural gas was the largest source of electricity (33.2%), followed by coal (28.7%), nuclear (19.9%), etc. (EIA, 2019c). Therefore, the CO_2 emission that an AET vehicle is responsible for can vary depending on the power sources in the area.

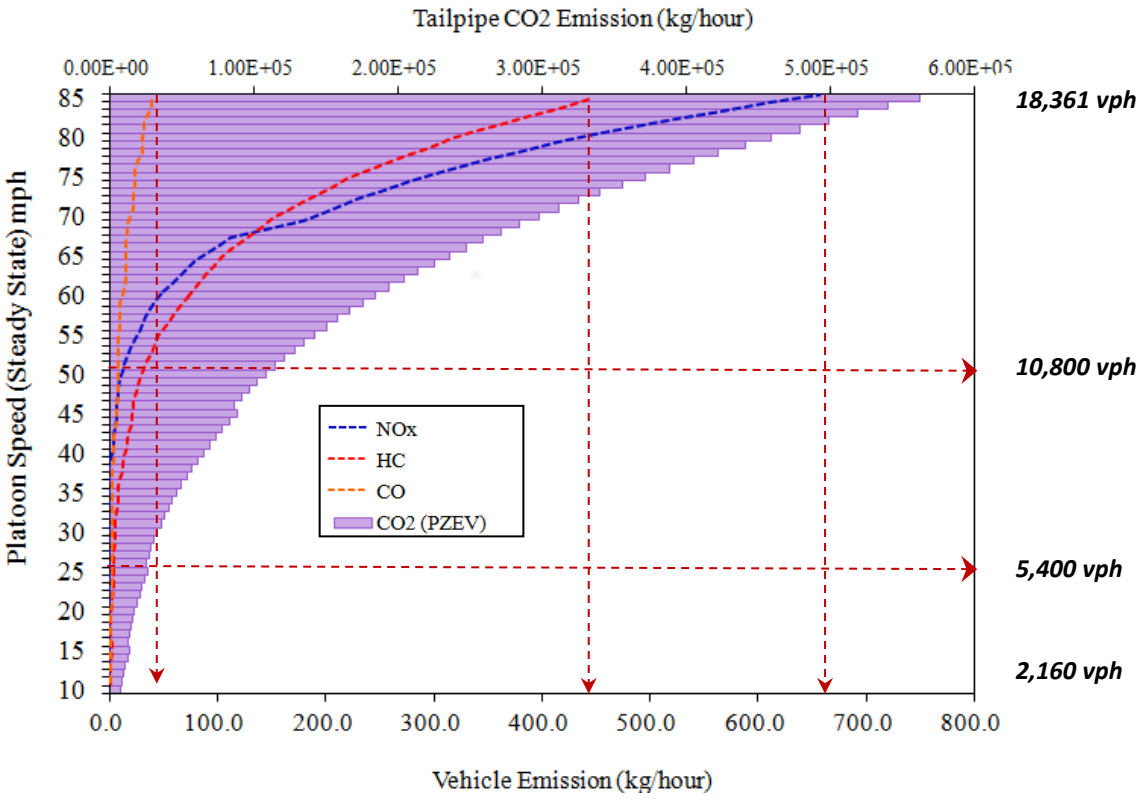

Figure 14 Tailpipe emissions of HC, NO_x, CO_2, and CO

Table 3 CO_2 emission intensity for AET and manual control systems (for a 10-vehicle platoon)

System	Power Sources/Technology	CO_2 emission intensity (gram CO_2/kWh) (Sovacool, 2008.)	CO_2 emission intensity (gram CO_2/km)
AET System	**Wind**	**10**	**54.3**
	Biogas	11	59.8
	Solar Power	13	70.6
	Nuclear	66	358.6
	Natural Gas	443	2,407.0
	Diesel	778	4,227.3
	Coal	**960**	**5,216.1**
Manual Control	Internal Combustion Engine	CMEM Model Toyota Camry*	786.6

** Based on super ultra-low emission vehicle/partial zero emission vehicle (vehicle category 27, CMEM)*

The emissions of one AET platoon can vary from very low (i.e., 54.3 grams CO_2/km generated by wind power source**)** to very high (i.e., 5,216.1 grams CO_2/km generated by coal). The emission of the conventional ICE vehicles in this study is about 786.6 CO_2 gram/km. Results from the emission analysis indicate the range of CO_2 reduction. This is because they vary considerably depending on the power sources used to generate electricity. It requires a comprehensive understanding of the grid power generation characteristics and prediction of how the grid technology evolves in order to respond to an increasing AET demand in the future.

5. Conclusion and future research

In this study, an evaluation framework was developed for estimating the benefits of AET system. The key findings and conclusions of this study are summarized as follows:

- The car following, merging and diverging models for AET were developed using the API in the microscopic simulation model. The vehicle activity profiles for AET and manual control systems were obtained from the microscopic simulation model and the simulated profiles were generated to further analysis of capacity, energy consumption and emission in the evaluation framework. Three measures of effectiveness, including system capacity, energy saving, and environmental emission reduction, were considered in the evaluation framework of AET system.
- The results of system capacity models derived from the simulation model agree with those obtained from the analytical model. The merging and diverging models were developed to replicate the real-world capacity reduction of the mainline and could possibly be adopted for maintaining the effective operation of the mainline. In addition, the system capacity results indicate that there are substantial benefits to the AET concept.
- In addition, the platooning operations appear to offer the aerodynamic advantage as they create the drafting effect when vehicles traveling at close spacing, and ultimately reduce the energy to overcome certain resistant forces. The experiments of battery only model indicate the possible range of AET vehicles within the urban area or city range. However, for interstate trips, it is necessary for the AET system to install the WPT system in order to prolong the travel distance. The experiment indicates that the AET vehicles can travel along the AET lane with a WPT efficiency of at least 90% without the need to stop for recharging.

- The benefits in terms of environmental emission reduction are debatable. This is because they vary considerably depending on the power sources used to generate electricity. It requires a comprehensive understanding of the grid power generation characteristics and prediction of how the grid technology evolves in order to respond to an increasing AET demand in the future.

With the development of connected, automated, and electric vehicles, and dynamic wireless charging technologies, the AET system is on the horizon. The proposed evaluation framework can help decision makers quantify the benefits of the AET system and make informed decisions in deploying such a system. The evaluation framework provides the effectiveness result of the project with clear indicators, baselines, and approach for quantifying the system's benefits. It could help the organization to evaluate whether the proposed system is suitable for investment, and how future highway infrastructure might be improved.

Further research should be carried out to better characterize the AET system and evaluation framework as follows:

- Platoon operations associated with merging and diverging operations should be modified to be able to capture the negative impacts of platoon splitting and re-forming. Truck platoon and the large vehicle mixing rates in the passenger platoon should be further investigated in the simulation model.
- The future evaluation framework should consider the impact of system control malfunction or communication lagged effect that may result in a larger intra-platoon distance so that it could prevent the collision. As a result, it could also degrade the AET performance measures (i.e., capacity, energy, and emission).
- Various effects that can substantially affect the AET system performance should be further investigated. They are, for instance: the effects of mixed autonomous and conventional vehicles in the AET system and peripheral networks, like a study by Wu et al. (2020), the centralized traffic flow management that control the mixture and routes of two vehicle types so that we can achieve the system optimal (SO) (Chen et al., 2020).

These further studies can help to improve the assessment of AET performance measures to better support future investments. Ultimately, this evaluation framework can provide a roadmap for future AET deployment.

References

American Energy Independence, 2019. Journey to Energy Independence. Available via: http://americanenergyindependence.com/ [Accessed August, 2019].

Advancing Sustainability through Powered Infrastructure for Roadway Electrification (ASPIRE) (2020, October 15). ASPIRE Research. Retrieved from https://aspire.usu.edu/about/research.

Bando, M., Hasebe, K., Nakayama, A., Shibata, A., Sugiyama, Y., 1995. Dynamic model of traffic congestion and numerical simulation. Physical Review E 51, 1035.

Barth, M., An, F., Younglove, T., Scora, G., Levine, C., Ross, M., Wenzel, T., 2000. The development of a comprehensive modal emissions model. NCHRP Web-only document, 122, 25-11.

Boys, J. T., Covic, G. A., Elliott, G. A. J., 2002. Pick-up transformer for ICPT applications. Electronics Letters 38(21), 1276-1278.

Browand, F., Zabat, M., Tokumaru, P., 1996. Aerodynamic benefits from close-following. Automated Highway Systems, Editted by Petros A. Ioannou. Plenum Publishing Corporation, New York.

Budhia, M., Covic, G. A., Boys, J. T. 2009. Design and optimisation of magnetic structures for lumped Inductive Power Transfer systems. in IEEE Energy Conversion Congress and Exposition, 2009. ECCE 2009., 2081-2088.

Center for Sustainable Electrified Transportation (SELECT), 2020. About Research. Available via: https://select.usu.edu/research/index. [Accessed July 2020].

Choi, S., Huh, J., Lee, W. Y., Lee, S. W., Rim, C. T., 2013. New cross-segmented power supply rails for roadway-powered electric vehicles. IEEE transactions on Power Electronics 28(12), 5832-5841.

Chakroborty, P., Das, A. 2005. Principles of Transportation Engineering. Prentice Hall.

Chandler, F. E., Herman, R., Montroll, E.W., 1958. Traffic dynamics: Studies in car following. Operations Research 6, 165-184.

Chen, L., Nagendra, G. R., Boys, J. T., Covic, G. A., 2015. Double-coupled systems for IPT roadway applications. IEEE Journal of Emerging and Selected Topics in Power Electronics 3(1), 37-49.

Chen, Z., Liu, W. and Yin, Y., 2017. Deployment of stationary and dynamic charging infrastructure for electric vehicles along traffic corridors. Transportation Research Part C: Emerging Technologies 77, 185-206.

Chen, Z., Lin, X., Yin, Y. and Li, M., 2020. Path controlling of automated vehicles for system optimum on transportation networks with heterogeneous traffic stream. Transportation Research Part C: Emerging Technologies 110, 312-329.

Chen, Z., Yin, Y., Song, Z., 2018. A cost-competitiveness analysis of charging infrastructure for electric bus operations. Transportation Research Part C: Emerging Technologies 93, 351-366.

Cirimele, V., Freschi, F., Guglielmi, P., 2014. Wireless power transfer structure design for electric vehicle in charge while driving. Electrical Machines (ICEM), 2014 International Conference on IEEE, 2461-2467.

Covic, G. A., Elliott, G., Stielau, O. H., Green, R. M., Boys, J. T., 2000. The design of a contact-less energy transfer system for a people mover system. Power System Technology, 2000. Proceedings. PowerCon 2000. International Conference on IEEE, 1, 79-84.

Fagnant, D. J., Kockelman, K., 2015. Preparing a nation for autonomous vehicles: opportunities, barriers and policy recommendations. *Transportation Research Part A: Policy and Practice 77*, 167-181.

Fishelson, J., Heaslip, K., Louisell, W., Womack, K., 2011a. An Evaluation Framework for an Automated Electric Transportation Network. In the Proceedings of the 90th Transportation Research Board Annual Meeting, Washington, DC, January 2011.

Freckleton, D., Fishelson, J., Heaslip, K., 2011b. Human Factors and Safety Challenges in the Transition to an Automated Electric Transportation System. 2011 Intelligent Transportation Systems World Congress, Orlando.

Fuller, M., 2016. Wireless charging in California: Range, recharge, and vehicle electrification. Transportation Research Part C: Emerging Technologies 67, 343-356.

Ghiasi, A., Hussain, O., Qian, Z. S., Li, X., 2017. A mixed traffic capacity analysis and lane management model for connected automated vehicles: A Markov chain method. Transportation Research Part B: Methodological 106, 266-292.

Gipps, P. G., 1981. A behavioural car-following model for computer simulation. Transportation Research Part B: Methodological 15(2), 105-111.

Heaslip, K., Womack, K., Muhs, J., 2011. Automated electric transportation: a way to meet America's critical issues. Leadership and Management Engineering 11(1), 23-28.

Horowitz, R., Varaiya, P., 2000. Control Design of an Automated Highway System. Research Report by the California PATH Program and the National Science Foundation. University of California, Berkeley.

Huang, C. Y., Boys, J. T., Covic, G. A., Budhia, M., 2009. Practical considerations for designing IPT system for EV battery charging. 2009 IEEE Vehicle Power and Propulsion Conference. IEEE, 402-407.

Huh, J., Lee, S. W., Lee, W. Y., Cho, G. H., Rim, C. T., 2011. Narrow-width inductive power transfer system for online electrical vehicles. IEEE Transactions on Power Electronics 26(12), 3666-3679.

Jang, Y. J., 2018. Survey of the operation and system study on wireless charging electric vehicle systems. Transportation Research Part C: Emerging Technologies 95, 844-866.

Johnston, R., A., Ceerla, R., 1993. A Continuing Systems-level Evaluation of Automated Urban Freeways: Year Three. Research Reports, California Partners for Advanced Transit and Highways (PATH), Institute of Transportation Studies (UCB), UC Berkeley.

Kanaris, A., 2010. Spacing and Capacity Evaluations for Different AHS Concepts Automated Highway Systems. Chapter in Automated Highway Systems. Springer.

Kissin, M.L.G., Covic, G.A., Boys, J.T., 2008. Estimating the output power of flat pickups in complex IPT systems. Proc., 39th Power Electronic Specialists Conference, Rhodes, Greece, 604.

Kometani, E., Suzaki, T., 1958. On the stability of traffic flow. J. Operations Research, Japan 2, 11-26.

Krauss, S., Wagner, P., Gawron, C., 1997. Metastable states in a microscopic model of traffic flow. Physical Review E 55, 5597.

Lee, D-H., Yang, X., Chandrasekar, P. 2001. Parameter optimization for Paramics using a genetic algorithm. Transportation Research Board, Washington, D.C. January 2001.

Leutzbach, W. 1988. An Introduction to the Theory of Traffic Flow. Springer-Verlag, Berlin, Germany.

Li, S., Mi, C. C., 2014. Wireless power transfer for electric vehicle applications. IEEE Journal of Emerging and Selected Topics in Power Electronics 3(1), 4-17.

Liu, Y., Guo, J., Taplin, J., Wang, Y., 2017. Characteristic analysis of mixed traffic flow of regular and autonomous vehicles using cellular automata. Journal of Advanced Transportation 2017, Article ID 8142074.

Limb, B. J., Crabb, B., Zane, R., Bradley, T. H., Quinn, J. C., 2016. Economic feasibility and infrastructure optimization of in-motion charging of electric vehicles using wireless power transfer. In Emerging Technologies: Wireless Power Transfer (WoW), 2016 Workshop on IEEE PELS, 42-46.

Liu, Z., Song, Z., 2017. Robust planning of dynamic wireless charging infrastructure for battery electric buses. Transportation Research Part C: Emerging Technologies 83, 77-103.

Liu, Z., Song, Z., He, Y., 2017. Optimal Deployment of Dynamic Wireless Charging Facilities for an Electric Bus System. Transportation Research Record: Journal of the Transportation Research Board (2647), 100-108.

Mahmassani, H. S., 2016. 50th anniversary invited article—autonomous vehicles and connected vehicle systems: flow and operations considerations. Transportation Science 50(4), 1140-1162.

McAuliffe, B.R., Croken, M., Ahmadi-Baloutaki, M., Raeesi, A., 2017. Fuel-economy testing of a three-vehicle truck platooning system. Technical report, NRC Report LTR-AL-2017-0008, National Research Council Canada.

Morris, C., 2015. Utah State University builds a dynamic wireless charging test track (2015) Available via: http://chargedevs.com/features/utah-state-university-builds-a-dynamic-wireless-charging-test-track/ [Accessed August 23, 2019].

Nagel, K., Schreckenberg, M., 1992. A cellular automaton model for freeway traffic. Journal de Physique I. 2(12), 2221.

National Research Council, 2010. Transitions to Alternative Transportation Technologies—Plug-in Hybrid Electric Vehicles. Washington, DC: The National Academies Press. https://doi.org/10.17226/12826.

Newell, G.F., 2002. A simplified car-following theory: a lower order model. Institute of Transportation Studies, University of California, Berkeley.

PATH team, 1996. Roadway Powered Electric Vehicle Project Parametric Studies: Phase 3D Final Report. California Partners for Advanced Transit and Highways Research Report.

Rothery, R. W., 1992. Car Following Models, in Revised Monograph on Traffic Flow Theory., Ch. 4. Available via: http://www.fhwa.dot.gov/publications/research/operations/tft/ [Accessed August 23, 2019].

Suh, N. P., Cho, D. H., Rim, C. T., 2011. Design of on-line electric vehicle (OLEV). In Global Product Development. Springer Berlin Heidelberg, 3-8.

Sovacool, B.K., 2008. Valuing the greenhouse gas emissions from nuclear power: A critical survey. Energy Policy 36, p. 2950.

Transportation Research Board (TRB), 2016. Highway Capacity Manual, Sixth Edition: A Guide for Multimodal Mobility Analysis. Washington, D.C.

Transportation Research Board (TRB), 1998. "Special Report 253: National Automated Highway System Research Program, A Review", Transportation Research Board; Washington, DC (1998).

Treiber, M., Hennecke, A., Helbing, D., 2000. Congested traffic states in empirical observations and microscopic simulations. Physical Review E 62(2), 1805.

U.S. Department of Energy, Energy Information Administration (EIA), 2019a. Monthly Energy Review. Available via: http://www.eia.gov/totalenergy/data/monthly [Accessed August 23, 2019].

U.S. Department of Energy, Energy Information Administration (EIA), 2019b. Oil, Crude, Petroleum Product, Explained (2017 data). Available via: http://www.eia.gov/energyexplained/index.cfm?page=oil_home#tab3 [Accessed August 23, 2019].

U.S. Department of Energy, Energy Information Administration (EIA), 2019c. Electric Power Monthly. Available via: http://www.eia.gov/electricity/monthly/ [Accessed August 23, 2019].

U.S. Environmental Protection Agency (EPA), 2019. Fast Facts on Transportation Greenhouse Gas Emissions. Available via: https://www.epa.gov/greenvehicles/fast-facts-transportation-greenhouse-gas-emissions [Accessed August 23, 2019].

Varaiya, P., 1993. Smart cars on smart roads: Problems of control. IEEE Transactions on Automatic Control 38(2), 195-207.

Wu, W., Zhang, F., Liu, W., Lodewijks, G., 2020. Modelling the traffic in a mixed network with autonomous-driving expressways and non-autonomous local streets. Transportation Research Part E: Logistics and Transportation Review 134, 1-22.

Appendix A: Pseudo Code for AET System Simulation

Platoon Forming

```
If (following vehicle on platoon forming link; check presence of following vehicle)
{Compute the speed of lead vehicle and following vehicle
   Compute gap distance at time t
        If (vehicle is not lead vehicle or platoon leader)
            Compute the desire deceleration rate for inter-platoon gap distance
        Else
            Compute the desire deceleration rate for intra-platoon gap distance
        End if
Compute the speed of following vehicle for next time interval (t+T)}
End if
```

Gap Detection

```
If (vehicle is on the checking point for gap acceptance)
{       If (vehicle == tail vehicle of a platoon)
        Compute gap distance of the behind vehicle
        End if
        Compute the number of vehicle allowed for the gap distance
        rampopen=true
}
End if
```

Lane Changing for Merging to AET System

```
If (rampopen)
{       for (count=1 to the number of allowed vehicles)
        {       If (vehicle is on ramp)
                count=count +1
                Else    break
                End if
        }
        rampopen=false
}
End if

If (entering vehicle on merging side link)
{Accelerate the speed
If (vehicle is on merging point)
        Change the lane to main lane
        Else
                Keep the same lane
        End if
}
End if
```